J. Membrane Biol. 11, 57–74 (1973)

An Analysis of Flash-Induced Electrical Transients of a BLM Containing Chloroplast Lamella Extracts

H. Ti Tien and J.S. Huebner*

Department of Biophysics, Michigan State University, East Lansing, Michigan 48823

Received 1 June 1972

Summary. The electrical transients produced by chloroplast bilayer lipid membranes (Chl-BLM) from flash excitation are seen to result from three photocurrents and a discharge current. Each of the three photo-initiated charge transports in Chl-BLM (designated as Components A, B and C) exhibits an action spectrum similar to chlorophyll absorption spectra. The fast components (A and B), which are induced by electron acceptors such as Fe^{+3}, have rise-times of ~ 3 μsec and ~ 20 msec, and occur in TLM (thin lipid membranes, i.e., colored membranes up to ~ 1 μ thick) as well as in BLM. Component C is induced by a transmembrane pH difference or applied voltage, has a rise-time of ~ 1 sec, and occurs only in BLM. Component C is associated with exciton dissociation and proton transport. The mobility of the Component A current carriers in TLM is estimated to be about 1×10^{-2} cm^2/volt sec, and are, hence, *electronic*. The photovoltage waveforms are described by equations developed, which consider Component A as being caused by a direct charge separation proportional to the illumination intensity (within $\gtrsim 0.5$ μsec), and Components B and C being caused by two types of exciton processes which cause charge transport after the illumination period.

Evidence derived from electron-microscopy, X-ray diffraction, and birefringence as well as circular dichroism studies strongly indicates that the photosynthetic apparatus is composed of highly organized lamellar structure. For instance, a model of a chloroplast thylakoid membrane depicted by Mühlethaler (1966) consists of two protein layers separated by a Gorter-Grendel bilayer of lipids. Other models have been proposed by Menke (1967) and by Benson (1966). The salient features in all these models lie in their oriented lipid core onto which other important cellular constitutents such as proteins may interact through either ionic or van der Waals attraction or both. Within the chloroplast, the usual picture is that a granum is composed of an ordered array of lamellar membranes. Each lamellar membrane is believed to separate two phases forming the so-called inner

* *Present address:* Natural Sciences Department, University of North Florida, Jacksonville, Florida 32216.

and outer spaces. The thickness of this thylakoid membrane is estimated to be about 70 to 120 Å (for a review, *see* Branton, 1969). However, the intrinsic complexity and often unfavorable geometry and size of the biological membranes have hindered many physical studies of their properties. The introduction of the bilayer lipid membrane by Mueller, Rudin, Tien and Wescott (1962; *see also* Tien, 1971) has provided a convenient artificial membrane system which can be modified to mimic many of the properties attributed to important biological membranes. The attractiveness of the experimental bilayer lipid membranes (hereafter abbreviated BLM) as a model system lies in the dimensional, electrical, permeability, and "excitability" characteristics which they possess and which correspond to some extent to those of biological membranes (Tien, 1972*a*). The light-induced excitability of pigmented BLM is of particular interest from the standpoint of photosynthesis and vision.

In a short communication, we have recently reported the electrical transients of BLM formed from chloroplast lamella extracts elicited by light flashes (Huebner & Tien, 1972). In the present paper, we present the results of further experiments with chloroplast BLM using flash excitation and interpret the findings of this and previous work in terms of exciton dissociation kinetics (*cf.* Kobamoto & Tien, 1971).

Materials and Methods

The laboratory distilled water was re-distilled in an all-glass apparatus (Model AG-la, Corning Glass Works) before use. The chemicals and solvents were reagent grade and were used as obtained. Fresh spinach leaves obtained from a local supermarket were washed and had their stalks and midribs removed before use. The chloroplast BLM-forming solution was prepared as previously described (Van & Tien, 1970). Membrane-forming solutions for TLM (i.e., thin lipid membranes exhibiting interference colors) were usually prepared with three parts by volume dodecane to one part butanol, while solutions for BLM formation were prepared with equal parts. Higher ratios of dodecane resulted in lower membrane-thinning rates, and often higher membrane resistance values, but no other changes were observed. Test solution pH values near 5.5 and the presence of ferric ions also were helpful in retarding the membrane-thinning process.

The exprimental arrangement for membrane measurements is illustrated in Fig. 1. A circuit for applying various values of voltage and shunt resistance between the calomel electrodes described elsewhere was used (Tien & Howard, 1972). Briefly, a mercury cell was connected through an on-off reversing switch to a potentiometer; one side of the potentiometer connected to the common electrode, the other side connected through a resistor (1% Hi-meg Resistors, Victoreen Instrument Co.) to the cup (+) electrode. The value of the shunt resistor R_s used will be specified in each case. By observing the variation in the membrane voltage $V(t)$ when a known voltage V_0 was applied or removed, the membrane dark resistance R_m and capacitance C_m were determined in the usual manner (Tien & Howard, 1972).

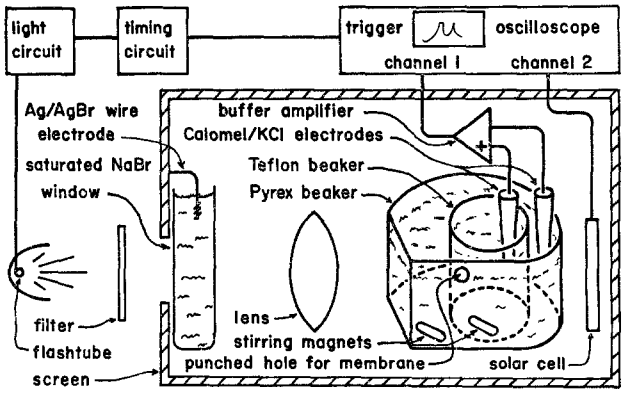

Fig. 1. Experimental arrangement for studying flash-induced electrical transients in pigmented BLM

The buffer amplifier was constructed using a field-effect transistor-input operational amplifier (Model 1021, Teledyne-Philbrick/Nexus Co.) to provide unit gain. The input impedance was $\sim 7 \times 10^{11}\ \Omega$. Calomel electrodes with shortened leads were connected to the buffer amplifier inputs and to the two aqueous solutions. The buffer amplifier and electrodes input capacitance was determined by the discharge method to be ~ 8 pF; the standard Teflon cup had a capacitance of about 50 pF (Tien & Howard, 1972). Typically, the BLM capacitance was greater than 5,000 pF, so the cup and buffer amplifier shunt capacitance could be ignored when dealing with BLM. A thick-walled Teflon cup, with a $\sim$2-mm diameter drilled hole, was used for the TLM measurements. This cup had a capacitance of about 3 pF. The outside solution (in the Pyrex chamber) was grounded through one calomel electrode (the common electrode); this arrangement reduced the electrical noise by shielding the inside solution with the grounded outside solution.

The membranes were formed by depositing approximately 2 μliters of the membrane-forming solution from a microsyringe with a repeating dispenser (Tien & Howard, 1972). BLM were observed to thin to the black state using dim green light before any asymmetrical conditions were established. The asymmetrical conditions used in the TLM cases were usually established within a few minutes after membrane formation. The chemical or pH differences across the membrane were established by removing a small volume of solution from the inner cup and replacing it with an equal volume of the concentrated solution of the chemical to be studied ($FeCl_3$, HCl, KOH, etc.). This procedure was accomplished by using a micropipette (Sampler, Oxford Laboratories), and was followed by magnetic stirring for a 10- to 15-min period in the dark. After applying a voltage, a brief period ($\sim$2 min) was allowed for the system to reestablish equilibrium before recording a photo-response.

A transistorized circuit was used to initiate the oscilloscope sweep prior to triggering the light flashes. The stroboscope (Model 1539-A, General Radio Company) used a xenon flash-tube; the light intensity was estimated to be about 10^9 lux, with the 1/3 intensity points being separated in time by about 3 μsec (Kobamoto & Tien, 1971). In some experiments neutral density filters (Carl Zeiss, Inc.) were used to reduce the light intensity. Red, green and blue color filters (Edmund Scientific Company) were also used. A photo-transistor (2N5779, General Electric Company) and a silicon solar cell (Edmund Scientific Co.) were used to record the light intensity variations. The photo-transistor

circuit measured the light intensity directly; the solar cell circuit was arranged to provide the time integral of the light intensity plus a much slower discharge curve.

Since the stroboscope used produces light by an arc discharge across electrodes in the xenon flash-tube, a burst of transmitted radio frequency energy accompanies such discharges, and appears as radio frequency noise in adjacent and unshielded circuits. Precautions were taken to reduce this noise by isolating the stroboscope from all other circuits, and by using a saturated saltwater window (a flask of saturated NaBr solution grounded to the Faraday screen cage with an Ag–AgBr wire electrode). In addition, the spacial orientation of the flash-tube electrodes was adjusted to provide minimum coupling with the buffer amplifier circuit. To ensure a proper and constant alignment, the arc's image was focused on the hole in the Teflon cup before membrane formation. Dim green light was used for observation during membrane formation.

Waveforms were displayed on a dual channel recording oscilloscope (Model R5031, Tektronix, Inc.). Traces were recorded by photographing the oscilloscope screen. A chart recorder (Model VOM 5, Bausch and Lomb) was connected in parallel with the oscilloscope and provided a record of the low speed variations in the membrane voltage and an accurate time history of the membrane under investigation.

Results

The dynamic performance of the calomel electrodes and buffer amplifier arranged for membrane voltage measurements was evaluated for small voltage variations by using a nonpunctured Teflon cup and driving the inner cup solution with a square-wave generator through a low-impedance Ag–AgCl wire electrode. The square-wave generator and buffer amplifier outputs were displayed directly on the oscilloscope. The results are illustrated in Fig. 2(*a*), where the square-wave rise-time may be seen to be ~ 0.3 μsec. The buffer amplifier output trace is seen to have a rise-time of ~ 0.5 μsec, with a comparable delay. This time delay is slightly greater than the product of the calomel electrodes resistance and the buffer amplifier input capacitance. From these traces, it is clear that the output of buffer amplifier follows the electrical potential of the inner aqueous solution to within ~ 0.5 μsec.

The three asymmetrical conditions used to elicit photoresponses from the BLM were: (1) chemical concentration ΔC, (2) hydrogen ion concentration ΔpH, and (3) applied voltage, ΔV. The components of flash-induced waveforms are designated as follows: (*i*) Component A, a rapid change in the membrane voltage which occurs principally during the flash excitation; (*ii*) Component B, a slower change in voltage, which reaches a peak value in about 20 msec *after* the flash excitation; (*iii*) Component C, a much slower change compared with Component B; and (*iv*) Component D, the decay of the membrane voltage in the dark. Components A and B are induced by an electron acceptor such as $FeCl_3$ and have a polarity such as to make the electron acceptor side of the membrane negative. At pH values near 5.5, Components A and B transport nearly the same amount of electric charge,

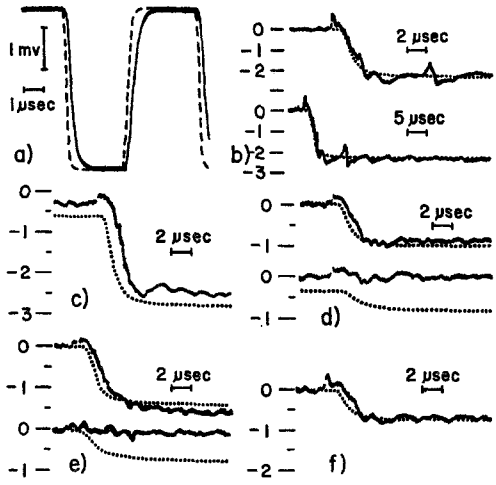

Fig. 2. The time course of output voltages: (*a*) The dynamic response of the calomel electrodes and buffer amplifier (solid line) to the square-wave voltage (dashed line) applied to the solution. (*b*) through (*f*) Component A membrane responses (solid lines) in 0.1 M acetate buffer at pH 5.5; one side of the bathing solution contained 2.5 mM $FeCl_3$. The simultaneous solar cell responses are shown in dotted lines. A 10^9 Ω shunt resistor was used in each case. (*b*) Successive traces of the Chl-BLM photovoltage waveform are shown with the solar cell response superimposed, at two recording speeds. (*c*) The response of another Chl-BLM with the solar cell trace offset. (*d*) The response of another Chl-BLM to unmodified light intensity (upper trace) and to green light (lower trace). (*e*) The response of Chl-TLM to unmodified light intensity (upper trace) and to green light (lower trace). (*f*) The response of another Chl-TLM. From capacitance measurements, the TLM thickness in (*e*) and (*f*) are inferred to be 0.4 and 0.3 μ, respectively. Flash duration $\simeq 3$ μsec

as determined by the relative voltage variations induced. Under these conditions, the Component B photocurrent is about 10^4 times smaller than the Component A photocurrent. A slow recorder response or dim, long duration illumination would probably mask the resolution of these photocurrents into their two separate components under either open-circuit voltage or short-circuit current conditions.

Component A photovoltage waveforms for Chl-BLM are illustrated in parts (*b*), (*c*), and (*d*) of Fig. 2. These high-speed traces were recorded simultaneously with the solar cell circuit output, which is closely proportional to the time integral of the light intensity. The oscilloscope amplifier gain was adjusted so that the solar cell trace had approximately the same deflection as Component A. The same gain settings were used on successive traces shown in Fig. 2(*d*) and (*e*), where in both cases the upper trace was recorded using white (unmodified xenon) light and the lower trace was recorded with the green filter inserted in the light path. The reduced deflec-

tion of the solar cell trace reflects the reduced light intensity. Only noise remains on the membrane voltage traces, since chlorophyll does not absorb green light. Comparable membrane voltage traces resulted when the light was completely blocked by a black plastic film, in which case no solar cell deflection was observed, and when white light was used with no ΔC asymmetry. Lower speed traces of the Chl-BLM photovoltage waveforms resulting from a variety of experimental conditions have been previously published (Huebner & Tien, 1972).

Fig. 2(*e*) and (*f*) illustrate the Component A response in Chl–TLM with capacitance values of 130 pF and 190 pF, respectively. Visual observation of these TLM indicated that the Plateau-Gibbs border occupied about half the area of the aperture, with the thin membrane portion being of nearly uniform reflectivity, and therefore of approximately uniform thickness. From these values, and assuming a dielectric constant of 4 (Tien & Diana, 1967), the average thicknesses were calculated to be 0.4 and 0.3 μ, respectively. It should be noted from Fig. 2 that Component A amplitude in Chl–BLM is comparable to the Component A amplitude in the Chl–TLM. In Chl–TLM over 1 μ thick, the amplitude of Component A was decreased to where it could no longer be distinguished from the residual flash-induced noise.

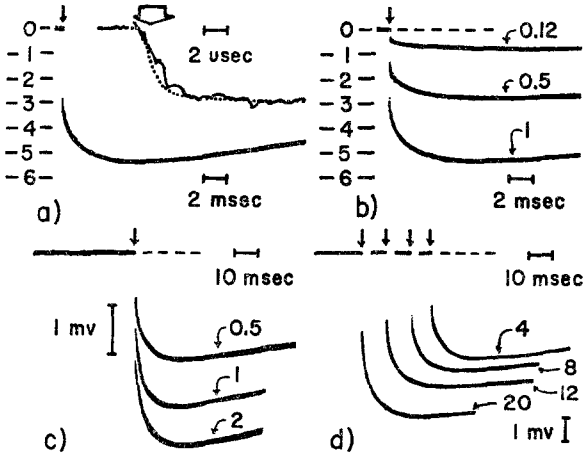

Fig. 3. Waveforms illustrating the Component A and B photoresponse of Chl–BLM induced by $FeCl_3$ and 3-μsec light flashes. Arrows mark the time of the flash excitation. A 10^8 Ω shunt resistor was used in each case. The solutions were 0.1 M propionate buffer at pH 5.5 in (*a*) and (*b*), and 0.1 M acetate buffer at pH 5.5 in (*c*) and (*d*). (*a*) The response (in mV) induced by a 1-mM $FeCl_3$ gradient. The upper part shows a high-speed trace superimposed with the solar cell response. (*b*) The response (in mV) of the same Chl–BLM used in part (*a*), to various values of illumination intensity, as labeled with 1 = 100%. (*c*) and (*d*) The response of a Chl–BLM to increased $FeCl_3$ concentrations as labeled with 0.5 = 0.5 mM $FeCl_3$

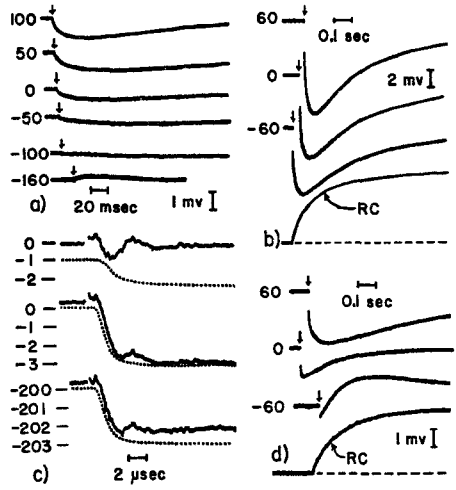

Fig. 4. The time course of the Chl-membrane photoresponse to 3-μsec light flashes. Arrows mark the time of the flash excitation when the solar cell trace (dotted line) is not shown. All membranes were formed in 0.1 M acetate buffer at pH 5.5, with 2.5 mM $FeCl_3$ added to one side after membrane formation. (*a*) Traces for a Chl–TLM about 1 μ thick (~55 pF) with various values of voltage applied through a 10^9 Ω resistor. The equilibrium dark voltage (in mV) precedes each trace. (*b*) Traces for a 0.3 μ thick (190 pF) Chl–TLM with initial dark voltage at 60, 0 and −60 mV. The voltages were applied through a 10^9 Ω resistor. The *RC* discharge which resulted from turning off the applied voltage is also shown. (*c*) High-speed traces of the same 0.3 μ thick Chl–TLM used in (*b*). The upper trace is with green light; the lower two traces are with unmodified xenon light and dark membrane voltages of 0 and −200 mV. (*d*) Traces for a Chl-membrane which contained both a colored (i.e., TLM) area and a black (i.e., BLM) area, with initial dark voltage at 60, 0 and −60 mV. The voltage was applied through a 10^8 Ω resistor. The membrane capacitance was ~2,000 pF. An *RC* discharge trace is also shown

Fig. 3(*a*) illustrates the Component A and B response for a Chl-BLM induced by 1 mM $FeCl_3$ added to one side of the bathing solution. Fig. 3(*b*) illustrates the response of the same Chl–BLM approximately 15 min later to various values of light intensity. The combined amplitude of Components A and B may be seen to increase linearly with the illumination intensity. High-speed traces showed that the amplitude of Component A also increased linearly with the illumination intensity. Fig. 3(*c*) and (*d*) show the effects of increasing the $FeCl_3$ concentration. A 15-min dark period was allowed after each addition of $FeCl_3$. The $FeCl_3$-induced voltage was compensated approximately by an applied voltage to cancel Component C. The amplitude of Component C, as measured at a fixed electrochemical gradient for protons, was increased by the additions of $FeCl_3$ to 2 mM, but was decreased at 12 and 20 mM. The dark membrane resistance was increased by the initial $FeCl_3$ addition, remained relatively constant to 12 mM, but was

reduced by about 50% with the addition of $FeCl_3$ to 20 mM. In addition, some precipitate was visible on the membrane at the 20 mM $FeCl_3$ concentration.

Fig. 4(*a*) shows that Component B still occurs in Chl–TLM ($\sim$1 μ thick) and may be modified by an applied voltage. The reversal of Component B above -100 mV should be noted. High-speed traces showed that Component A was $\lesssim$0.1 mV in amplitude. No photoeffects could be discerned from flash excitation for TLM of more than a few microns thick. Fig. 4(*b*) shows Components A, B and D for a Chl–TLM 0.3 μ thick, at several values of applied voltage. The reduced capacitance accounts for the relatively fast *RC* time. Part (*c*) of Fig. 4 shows that a -200 mV dark membrane voltage reduces the amplitude of Component A in a Chl–TLM by $\sim$25%, in contrast to the reversal of Component B at ~ -100 mV. In addition, Component A is seen not to be delayed in time by the negative voltage. Fig. 4(*d*) shows Components A, B, C and D for a Chl–TLM under similar conditions, except that it included a black area. Since the black area increased the membrane capacitance to $\sim$2,000 pF, a 10^8 Ω shunt resistor was used to reduce the *RC* time constant to near that of the Chl-TLM shown in Fig. 4(*b*). Comparison of the curves in Fig. 4(*b*) and (*d*) clearly shows the absence of Component C in the TLM. By observing waveforms during the membrane-thinning process, Component C was seen to appear concomitantly with the first black spot on the membrane, and increased in magnitude as the black area spread to form the BLM.

The photovoltage waveforms for a Chl–BLM which exhibited a particularly large Component C are illustrated in Fig. 5(*a*). The dark membrane resistance at -100 mV was 1.67×10^8 Ω and the capacitance was 8,000 pF. The amplitude of the photovoltage response increased linearly with the dark membrane voltage to -100 mV, and may be observed from Fig. 5 to increase with a less than linear rate above -120 mV. The peak photoresponse values also occur sooner after the flash excitation at higher voltage values. In addition, Component D may be seen to return the membrane voltage to the preillumination value more quickly in the higher voltage traces. Fig. 5(*b*) illustrates these details by superimposing the photovoltage waveforms of another Chl–BLM. Fig. 5(*c*) illustrates that the time at which Component C peak photovoltage value occurs following the light flash also varies with the illumination intensity. In contrast, the amplitude of Components A and B was seen to vary linearly with the light intensity, with virtually identical waveforms. Components A, B and C were also each seen to result from both red and blue light with nearly proportional amplitudes, but did not result from green light. Thus, the action spectrum

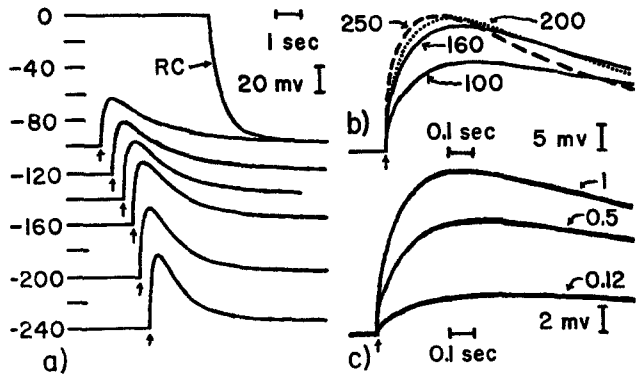

Fig. 5. The time course of the Component C response of Chl-BLM to 3-μsec light flashes. Arrows mark the time of the flash excitation. The BLM were formed in 0.1 M acetate buffer at pH 5.0 with 1 mM $FeCl_3$ present in the bathing solution prior to membrane formation. The voltages were applied through a 10^8 Ω resistor. (*a*) The membrane voltage trace showing the response when a voltage was applied to produce a −100 mV dark voltage (*RC*), and the photoresponse at various voltage values. (*b*) Superimposed photoresponses of another Chl-BLM showing the variations in the waveforms at various voltage values, as labeled (in mV). (*c*) The photoresponse of another Chl-BLM to various values of illumination intensity, as labeled, with 1 = 100%. The dark or pre-illumination voltage for each trace was −56 mV

for each component in the Chl-BLM is roughly that of the chlorophyll absorption spectrum (*cf.* Van & Tien, 1970).

The amplitude of Component C has previously been shown to increase with succeeding flash excitation, so that in some cases the response at the 11th flash was an order of magnitude larger than the initial response. After a 15-min dark period, the initial amplitude results. This effect has been observed only in 0.1 M buffer (in both acetate and propionate) near pH 6.0 and in the presence of $FeCl_3$. Recent investigations have shown that upon removing the applied voltage after the second flash and then reapplying it after the 10th flash, the amplitude of Component C to the 11th flash was unaltered from the expected result, had the voltage been continuously applied during all 11 flashes. The same amplitude enhancement results from the light flashes when the applied voltage polarity is reversed, or intermittently reversed.

Fig. 6(*a*) shows the photoresponse induced by a 1-mM ceric ammonium nitrate $[(NH_4)_2Ce(NO_8)_6]$ added to one side of the bathing solution. Note that the *RC* discharge compares closely with Component D after the flash excitation, and that Component B is nearly absent in this trace. This ceric salt induced larger Component B amplitudes in other BLM's, and reduced the dark membrane resistance of this membrane from 2.5×10^8 Ω to 9×10^7 Ω

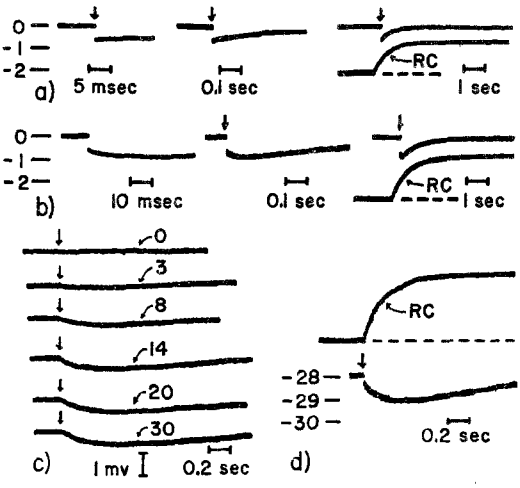

Fig. 6. Waveforms illustrating the photovoltage response of Chl-BLM as modified by other chemicals. Arrows mark the time of the 3-μsec fash excitation. (*a*) The response induced by 1 mM $(NH_4)_2Ce(NO_3)_6$ in 0.1 M acetate buffer at pH 5.0, shown at various sweep speeds. A 10^9 Ω shunt resistor was used; an *RC* discharge trace is shown. (*b*) The response of the same membrane used in (*a*), after the addition of 2.5 mM $FeCl_3$; both chemicals were added to the same side of the bathing solution. An *RC* discharge trace is also shown. (*c*) The response induced by a +50 mV dark voltage applied through a 10^8 Ω resistor. The initial trace (labeled 0) was recorded prior to the $K_2S_2O_8$ addition; the other traces were recorded at various times (as labeled in minutes) after $K_2S_2O_8$ was added to 2 mM strength in both solutions. The solutions were 0.1 M KCl at pH 6.5; the $K_2S_2O_8$ reduced the pH to ~6.2. (*d*) response of the same membrane used in (*c*), after adding 1 mM $FeCl_3$. The photoresponse was recorded with the applied voltage off, but with the 10^8 Ω resistor still shunting the membrane. The −28 mV dark voltage was produced by the $FeCl_3$ (a pH effect). Also shown is an *RC* discharge trace

within ~2 min. Part (*b*) of Fig. 6 shows the response of the same Chl-BLM after the addition of 2.5 mM $FeCl_3$ to the same side of the bathing solution. Note the larger Component B, and the longer *RC* discharge time, which again compares closely with Component D. In general, $FeCl_3$ has been found to increase the dark membrane resistance of Chl-BLM. In this case, the resistance increased to 2.4×10^8 Ω within ~2 min. Also, it was observed that the presence of $FeCl_3$ increases the speed (i.e., causes the peak to occur earlier in time) and amplitude of Component C in otherwise unmodified Chl-BLM. Similar effects were also detected with $(NH_4)_2Ce(NO_3)_6$.

The third compound investigated was potassium persulfate ($K_2S_2O_8$). This compound has been reported to quench the fluorescence of chlorophyll-containing BLM (Huebner, 1972). Fig. 6(*c*) shows the effects of potassium persulfate on our Chl-BLM. The addition of this compound to the bathing solution did not produce any unusual change in the membrane

resistance, but it did enhance the amplitude of Component C in about 15 min. (The Chl–BLM resistance did increase by ~10% in the 30-min period, but this increase is generally observed in Chl–BLM in the absence of $K_2S_2O_8$.) The Component C enhancement was observed under the same conditions as those reported for fluorescence quenching in chlorophyll-lecithin BLM. Three types of control experiments were performed in 0.1 M KCl at pH 6.5: (*i*) observing that Component C enhancement did not occur in 45 min under identical conditions but without $K_2S_2O_8$, (*ii*) observing that Chl–BLM prepared in previously mixed 2.5 mM $K_2S_2O_8$ solutions showed a comparable Component C amplitude enhancement, and (*iii*) observing that Chl–BLM which had been in contact with solutions containing $K_2S_2O_8$ for 30 min and Chl–BLM which had been aged for 30 min in solutions containing only KCl produced virtually identical photoresponses upon the addition of a 1-mM $FeCl_3$ gradient [*see* Fig. 6(*d*)]. Larger Component C responses were observed at lower pH values. The presence of 2.5 mM $K_2S_2O_8$ in either or both bathing solutions has been found to enhance the Component C response of Chl–BLM from 2 to 10 times in solutions of 0.1 M KCl and 0.1 M acetate buffer at pH 5.5, and in 0.1 M acetate buffer at pH 4.5, in all cases with the same ~15-min time period.

Discussion

The flash-induced photoeffects in these BLM's under asymmetrical conditions (ΔC, ΔpH, and ΔV) can be explained in terms of a simple model where the photoactive BLM is pictured as similar to a barrier-layer photovoltaic cell comprising a current generator in parallel with a resistance and a capacitance. It is also assumed that the incident radiant energy absorbed by the pigments in the BLM and its supporting Plateau-Gibbs border generates *electronic* charges *via* (*i*) direct electron emission and (*ii*) exciton dissociation (Tien, 1972*b*). The photogenerated electrons and holes drifting in the direction of existing fields can eventually effect reduction reactions on one side of the solution-BLM biface and oxidation reactions on the other side (Kobamoto & Tien, 1971).

Theory

As defined in the Results section, the time dependence of the photovoltage consists of four different phases which are designated as Components A, B, C and D, respectively. Component A is a rapid change in the membrane voltage which occurs principally during the flash excitation. Component B

is a slower change in voltage which reaches a peak value about 20 msec *after* the flash excitation. Component C is much slower as compared with either A or B, which lasts from several fractions of a second to seconds. Component D is the decay of the membrane voltage. Expressing these components in terms of transmembrane currents, the corresponding designations are: $i_A(t)$, $i_B(t)$, $i_C(t)$ and $i_D(t)$, respectively. The symbol t in the parentheses denotes time. These currents collectively alter the electrical charge on the membrane capacitance, each being present with amplitudes and polarity depending upon the experimental conditions. Since the Plateau-Gibbs border supports both BLM and TLM (i.e., thin lipid membranes showing colored fringes), the fact that Component C does not occur in TLM eliminates the possibility that it is a border effect. Furthermore, since the capacitance of a BLM may be over two orders of magnitude greater than that of a TLM, yet the amplitudes of the voltage change produced by Components A and B are comparable in the two types of membranes, the amount of charge transported by these components must vary nearly proportionally with the membrane capacitance and inversely with the membrane thickness. Thus, only a small fraction of Components A and B in BLM can result from the Plateau-Gibbs border. In this analysis, $V(t)$ shall represent the deviation of the membrane voltage from the dark equilibrium value, which may not be zero by virtue of pH differences or applied voltages. $i_D(t)$ is then given by,

$$i_D(t)=V(t)/R \tag{1}$$

where R is the effective transmembrane resistance, which is assumed not to vary with voltage. $V(t)$ may be expressed as

$$V(t)=Q(t)/C=(1/C)\int[i_A(t)+i_B(t)+i_C(t)-i_D(t)]\,dt. \tag{2}$$

Combining with Eq. (1), Eq. (2) becomes

$$\begin{aligned} V(t)&=(1/C)\exp(-t/RC)\int[i_A(t)+i_B(t)+i_C(t)]\exp(t/RC)\,dt \\ &=V_A(t)+V_B(t)+V_C(t) \end{aligned} \tag{3}$$

where

$$V_A(t)=(1/C)\exp(-t/RC)\int i_A(t)\exp(t/RC)\,dt, \quad \text{etc.}$$

Eq. (3) shows that the photovoltage waveforms may be represented as a sum of three component parts and their RC discharge. This separation of the waveform into independent components is possible only for small amplitude voltage variations, as we have shown experimentally that each of the components and thus their currents are modified by variations in the transmembrane voltage. By specifying the time variation of the three photo-activated currents in Eq. (3), it will be shown that the observed waveforms can be easily described.

First, we shall ignore for the time being $i_B(t)$ and $i_C(t)$ but assume that

$$i_A(t)=eN_A I(t) \tag{4}$$

where N_A is a proportionality factor and $I(t)$ is the illumination intensity. Since the RC time constant is always much greater than 3 μsec, Eq. (3) may be written as

$$V(t)=V_A(t)=(eN_A/C)\exp(-t/RC)\int_0^t I(t)\,dt. \tag{5}$$

Following the flash excitation, Eq. (5) becomes

$$V_A(t)=V_A\exp(-t/RC) \tag{6}$$

where V_A is designated as the amplitude of Component A.

In considering Components B and C, it is convenient to consider that the flash illumination is instantaneous and results in the formation of excitons. Discharging of the excitons will result in charge transport, provided suitable membrane asymmetries exist. We consider a model in which the current is controlled by the exciton dissociation rate. Letting $N(t)$ be the number of excitons, if the excitons dissociate by a single process at a rate $\lambda N(t)$ and cause one charge to be transported per exciton that dissociates, then an exciton photocurrent is given by

$$i_e(t)=e\lambda N(t)=e\lambda N^0\exp(-\lambda t) \tag{7}$$

where N^0 is the total number of excitons created by the flash illumination. This current will contribute a Component of the photovoltage, which is given by

$$\begin{aligned} V_e(t)&=\frac{e\lambda N^0}{C(\lambda-1/RC)}[\exp(-\lambda t)-\exp(-t/RC)] \\ &=V_e[\exp(-\lambda t)-\exp(-t/RC)] \end{aligned} \tag{8}$$

where V_e is the amplitude due to exciton dissociation.

Comparison with Experiments

Eq. (5) predicts that the Component A photovoltage will rise as the time integral of the illumination intensity, and fall as the RC discharge of the membrane in the dark. The solar cell and membrane photovoltage waveforms illustrated in Figs. 2, 4 and 6 demonstrate that to within 0.5 μsec, this is an accurate description of Component A in both BLM and TLM. Since any delay in the charge transport would shift Component A photovoltage later in time, we conclude that, within ~0.5-μsec illumination, exciting light can cause a capacitative current flowing across the membrane.

The fact that the transport time for Component A charge carriers in TLM approaching 1 μ thick is not further delayed from the BLM case is significant. If photogenerated ionic carriers are assumed to be driven across a 0.5-μ thick TLM in $\lesssim$0.5 μsec by an electrochemical gradient, the driving force must have a lower limit of $\sim$20 volts, owing to the limited mobility of ions in liquid hydrocarbons (Essex & Secker, 1968; Minday, Schmidt & Davis, 1971). This value is inconsistent either with Component A being induced by the presence of 1 mM ferric ion or with the variation of Component A amplitude as a function of applied voltages [*see* Fig. 4(*c*)]. Alternatively, if the driving force is set equal to the redox potential difference between the Fe^{+2}/Fe^{+3} and $H_2O/H,O_2$ couples ($\sim$400 mV), a lower limit on the charge carrier mobility of 1×10^{-2} cm^2 per volt sec results. This value is comparable to the measured values of free electron mobility in liquid hydrocarbons (Minday *et al.*, 1971), and confirms that Component A is electronic in nature. The failure of Component A to appear in TLM of more than 1 μ thickness is presumably because of very low membrane capacitance and the increased probability of electronic carriers encountering electron scavengers or traps in thicker membranes, a problem which does not interfere with the voltage generation in BLM. This explanation is also consistent with the view that Component A is electronic. The sign of the charge carrier (i.e., if they are electrons or holes) cannot be distinguished from these results, however. The photovoltage described by Eq. (8) is obtained by assuming that the charge transport occurs with a time much less than $1/\lambda$. Two modifications to this simple model are of interest: (*i*) The number of charges transported per exciton discharged may be less than one, but a fixed ratio. This modification would reduce the amplitude of the photocurrent and voltage component, but the component waveform will nonetheless be described by Eq. (8); (*ii*) Other exciton discharge processes which do not transport charge (e.g., fluorescence) may occur. If these other processes occur with a rate $\lambda' N(t)$, where $\lambda' \neq \lambda$, then the amplitude of the voltage component will be reduced, and λ in Eq. (8) must be replaced with a sum of the various λ's. Thus, the rate constant obtained from the waveform may not be that of the actual process effecting the charge transport. In both cases, the experimental data fitting into Eq. (8) will give N^0, the number of charges actually transported.

A significant point is that Eq. (8) accurately describes the Component B photovoltage waveforms observed in Chl-BLM. The trace shown in Fig. 3(*a*) is seen to fit to within $\sim$5% by using the following parameters in Eq. (6) for Component A and Eq. (8) for Component B: $V_A = 3$ mV, $V_B = 3$ mV, $1/\lambda_B = 1.75$ msec. The *RC* value was independently determined to be 0.07 sec.

A trace given earlier can be fitted by the following values: $V_A = 1.5$ mV, $V_B = 1.2$ mV, and $1/\lambda_B = 5$ msec. RC was 0.5 sec. (Component A response was limited by the rise-time of the buffer amplifier.) From this close agreement, we conclude that Component B in Chl–BLM results from the dissociation of excitons [*see* Huebner+Tien, 1972, Fig, 1 (*a*)].

Equation (8) is somewhat less successful when applied to Component B waveforms from Chl–TLM, and to Component C. For example, it is not possible to fit the 0 mV trace shown in Fig. 4(*b*) using Eqs. (6) and (8), and the measured RC value. If agreement is limited to providing the correct voltage amplitude at the peak value, the following parameters are obtained: $V_A = 4$ mV, $V_B = 27.5$ mV, and $1/\lambda_B = 50$ msec. The resulting theoretical curve fails to fit the experimental waveform in two ways; the theoretical voltage rises too slowly before the peak value, and falls too rapidly after the peak value. If the theoretical curve is made to fit the rising portion of the experimental curve, then it over-shoots the peak value, and still falls too rapidly. Attempts to fit Eq. (8) to Component C of the waveforms encounter similar difficulties. For example, the peak voltage value for the $I = 1$ trace in Fig. 5(*c*) is fit by using $V_C = 33$ mV and $1/\lambda_C = 0.2$ sec. Again, however, the theoretical curve rises too slowly before the peak, and falls too rapidly after the peak. Furthermore, the shifting of the peak voltage value in time with the illumination intensity clearly suggests that other variables alter the exciton dissociation rate for Component C.

It thus becomes of interest to consider possible physical processes which would require the waveform to be modified for Component B in TLM and Component C in BLM, and at the same time retain the agreement with experiment in the case of Component B in Chl–BLM. Since the dissociation rate constant for Component B in BLM is much greater than that for Component C, we conclude that two types of excitons must be involved in these photoeffects; one type activates Component B, and the other type activates Component C. Variations in the RC time caused by illumination-induced heating can be ruled out, as reduced resistance values and RC times would make the differences between the theoretical and experimental curves even larger. Variations in the membrane dynamic resistance are not likely to be the cause of the difference, as such variations (i.e., nonlinearities in the $I-V$ curve) do not generally appear below 100 mV. Variation in the exciton dissociation rate is most likely a cause of such waveform modification. The other causes that should be considered are: (*i*) time required for the excitons to diffuse to the discharge sites which is $\gtrsim 1/\lambda$; (*ii*) the presence of exciton traps which would delay the exciton migration and dissociation; (*iii*) the presence of traps which would delay the charge carrier transport for a time,

$\gtrsim 1/\lambda$; and (*iv*) the number of electron acceptor or other dissociation sites being less than the number of excitons, with the sites being exhausted or required to cycle with a time $\gtrsim 1/\lambda$. Any of these factors would result in a more complex waveform. In addition, other factors such as the solution pH, applied voltage, and specific chemicals have been shown to alter the amount of charge transported by each of the components, and may have a role other than its primary one. The diffusion of ions in the aqueous interface may also need to be considered (Tien, 1972*b*).

The success of Eq. (8) in describing Component B in BLM and its apparent failure in TLM provides an interesting caveat. In Chl–BLM, all of the pigments are in the two monolayers which make up the biface. Excitons created in the pigments can apparently either dissociate at their point of creation, or readily migrate in the compacted monolayer to their dissociation site. In TLM, however, the two monolayers are separated by a liquid hydrocarbon core which may contain more of the pigments than the two monolayers. The long characteristic time observed for Component B in the TLM [*see* Fig. 4(*b*)] may thus be caused by the time required for the excitons created in the liquid hydrocarbon core to reach their dissociation sites on the biface. In addition, competing processes which do not transport charge may be less effective in discharging the excitons within the core, so that the core may thus continue to supply excitons to the biface, and the apparent lower dissociation rate constant results in the waveform. This may result from the different molecular environment in the core and at the biface. It is also possible that molecules which are virtually excluded from the biface are present in the core. For whatever reasons, it appears likely that the lower rate constant in the waveforms for Component B in TLM results from excitons created within the core, which take longer to reach the dissociation sites on the biface. The lower amplitude of the response in the TLM apparently results from the processes which are less effective in charge transport. The liquid hydrocarbon core of the TLM apparently blocks Component C.

In certain experiments we have found that the presence of $FeCl_3$ in low concentration ($\sim 10^{-3}$ M) in 0.1 M acetate buffer increases the dark membrane resistance of BLM. From Eq. (8), increasing the resistance would be expected to increase the observed amplitude of Component C and cause the peak voltage value to occur later in time. The experimental results show that the amplitude is increased (often by many times), but the peak voltage value occurs earlier in time instead. This implies that the presence of $FeCl_3$ must increase the rate of Component C exciton dissociation to produce the charge carriers. Since the polarity and magnitude of Component

C depends upon the polarity and magnitude of the electrochemical potential for protons, it seems likely that, in the absence of such a potential, the charge carriers are still produced, but not transported. The presence of the potential only makes Component C observable, by transporting the charges. The increased rate of discharge in the presence of $FeCl_3$ or other chemicals may be sufficient to offset the loss of light energy to other processes which do not create charge carriers, such as fluorescence. Indeed, the presence of $K_2S_2O_8$ has been seen to enhance the Component C amplitude in Chl–BLM. Furthermore, $K_2S_2O_8$ and $FeCl_3$ are both seen to be nearly as effective in enhancing Component C in Chl–BLM when present in only one side of the bathing solution as when present in both sides. This suggests that the excitons dissociate more readily in membranes with a high chlorophyll content and that the excitons can migrate between the monolayers at the biface.

Conclusion

The role of photo-electrons and holes in coupled redox reactions on opposite sides of BLM have been previously considered (Tien, 1972*b*). In this work, we have provided further evidence of photo-electronic processes in lipid membranes, which strongly suggest that Component A in BLM is electronic. The results obtained in this study demonstrate that these processes must result in a transmembrane current (either capacitative or resistive or both) involving both the electrical double layers at the biface and the membrane. A simple exciton dissociation model is proposed which accurately describes the Component *B* waveforms in BLM and provides a basis for interpreting the variations observed in the Component B waveforms in TLM. This agreement, together with the fact that Component B, like Component A, is induced by electron acceptor gradients, suggests that Component B is also electronic in nature. The Component C waveforms are seen to be more complex, and are not fit by this model. The properties required for the excitons in generating Component B, apart from their long lifetime, are not different from those usually attributed to excitons in the chlorophyll-lamellar systems (Kamen, 1963).

H.T.T. is thankful to Dr. Victor K.H. Chen for helpful discussions.
This study was supported by a National Institute of Health Grant No. GM-14971.

References

1. Benson, A.A. 1966. On orientation of lipids in chloroplast and cell membranes. *J. Amer. Oil Chem. Soc.* **43**:265.
2. Branton, D. 1969. Membrane structure. *Annu. Rev. Pl. Physiol.* **20**:209.

3. Essex, V., Secker, P.E. 1968. Behavior of negative charge carriers in hexane. *Brit. J. Appl. Phys.* **1**:63.
4. Huebner, J.S. 1972. Quenched fluorescence of chlorophyll bilayer lipid membranes. *J. Membrane Biol.* **8**:403.
5. Huebner, J.S., Tien, H.T. 1972. Electrical transients of chloroplast bimolecular lipid membrane elicited by light flashes. *Biochim. Biophys. Acta* **256**:300.
6. Kamen, M.D. 1963. Primary Processes in Photosynthesis. Academic Press Inc., New York; and references therein.
7. Kobamoto, N., Tien, H.T. 1971. Light-induced electrical effects in a retinal bilayer lipid membrane. *Biochim. Biophys. Acta* **241**:129.
8. Menke, W. 1967. The molecular structure of photosynthetic lamellar systems. *Brookhaven Symp. Biol.* **19**:328.
9. Minday, R.M., Schmidt, L.D., Davis, H.T. 1971. Excess electrons in liquid hydrocarbons. *J. Chem. Phys.* **54**:3112.
10. Mueller, P., Rudin, D.O., Tien, H.T., Wescott, W.C. 1962. Reconstitution of excitable cell membrane structure in vitro. *Circulation* **26**:1167.
11. Mühlethaler, K. 1966. The ultrastructure of the plastid lamellae. *In:* Biochemistry of Chloroplasts. T.W. Goodwin, editor. p. 49. Academic Press Inc., New York.
12. Tien, H.T. 1971. Bimolecular lipid membranes: A review and a bibliography. *In:* Surface and Colloid Science, E. Matijevic, editor. Vol. 4, p. 361. John Wiley & Sons, Inc., New York.
13. Tien, H.T. 1972*a*. Membranes: Their interfacial chemistry and biophysics. *In:* Biennial Review of Surface Chemistry and Colloids. M. Kerker, editor. p. 11. MTP International Review of Science, Butterworths & Co., Ltd., London; University Park Press, Baltimore, Maryland.
14. Tien, H.T. 1972*b*. Electronic processes and photosensitization in bilayer lipid membranes. *Photochem. Photobiol.* **16**:271.
15. Tien, H.T., Diana, A.L. 1967. Black lipid membranes in aqueous media: The effect of salts on electrical properties. *J. Colloid Interface Sci.* **24**:294.
16. Tien, H.T., Howard, R.E. 1972. Techniques of BLM. *In:* Techniques of Surface Chemistry and Physics. R.J. Good, R.R. Stromberg, and R.L. Patrick, editors. Vol. 1, p. 109. Marcel Dekker, Inc., New York.
17. Van, N.T., Tien, H.T. 1970. Black lipid membranes in aqueous media: Photoelectric spectroscopy. *J. Phys. Chem.* **74**:3559.